PAPER • OPEN ACCESS

Non-linear buckling analysis of ship hull stiffened panels

To cite this article: E Hacihamud *et al* 2023 *IOP Conf. Ser.: Mater*. *Sci. Eng.* **1294** 012030

View the article online for updates and enhancements.

Non-linear buckling analysis of ship hull stiffened panels

E Hacihamud[1*], K Dahl[2], O Gabrielsen[2], H G Lemu[1] and S C Siriwardane[1]

[1] Department of Mechanical & Structural Engineering and Materials Science,
University of Stavanger, Norway
[2] Department of floating structures, DNV AS, Stavanger, Norway

*Contact author: enesalhh@gmail.com

Abstract. Stiffened panels are crucial in maritime applications, where buckling is a primary structural failure concern. Typically, assessing the buckling capacity of these panels relies on established guidelines like DNV-RP-C201 and NS-EN 1993-1-5. Alternatively, non-linear finite element methods, guided by DNV-RP-C208, can be used. However, there's a significant research gap in calibrating buckling capacities for large ship-hull stiffened panels. This paper bridges that gap by employing non-linear finite element analysis to evaluate the buckling capacity of ship hull stiffened panels and compare the results with DNV-RP-C201. It establishes a capacity benchmark by thoroughly comparing results for a plated panel. Subsequently, it develops a validated model using ABAQUS, introducing material and geometric nonlinearities, including a mid-stiffener span imperfection ranging from 0.06% to 1% of the stiffener span length for 99.7% calibration. The validated non-linear model then assesses the impact of holes on buckling capacity under uniaxial and gravity loads, revealing a clear correlation between reduced buckling capacity.

1. Introduction

Stiffened panels find widespread applications across various industries, with a particular emphasis on offshore and maritime sectors. Their popularity stems from their exceptional capacity to withstand heavy loads while maintaining a favorable stiffness-to-weight ratio. Given that buckling represents a prevalent failure mode in stiffened panels, extensive research efforts have been dedicated to its study over the years. This research encompasses analytical approaches, experimental testing, and the utilization of non-linear finite element (NLFE) methods.

Several standards such as DNV-RP-C201 [1] and NS-EN 1993-1-5 [2] provide design guidelines against failure by buckling. Based on recommendations of these and similar standards, it is possible to predict failure capacities of plated structures, though the scope of these standards may not be included in some cases, where instead NLFE can be used to determine the buckling capacity. DNV-RP-C208 [3] is a standard developed by NLFE as a recommended practices for this last case.

As real stiffened panels have geometrically imperfections introduced from fabrication methods and tolerances, introducing equivalent geometric imperfections in order to predict the buckling capacity correctly. The DNV-RP-C208 [3] recommended practice provides guidance to geometric imperfection amplitudes. It is concerned with identifying the characteristic resistance of a structure or section of a structure to meet the DNV criteria for ultimate strength in DNV recommended practices DNV-RP-C201 [1].

Conducting non-linear buckling analysis using recommendations of DNV-RP-C208 [3] does not imply that the aim is to replace the determination of structural buckling resistance compared with the

traditional standards, but to address the cases that are not within the limitations of the standards. It is crucial to consider the statistical variation of the different parameters, when using NLFE method to determine buckling resistance. This can be achieved by comparing the FE capacities with experimental capacities if physical testing could be performed.

In the past years, a significant amount of research has been conducted on the development and formulation of the ultimate limit strength for buckling capacities. Paik et al. [4] derived sets of such formulations for the steel plate elements that are under four load components such as compression/tension, edge shear, and lateral pressure loads assuming that the plates are simply supported along all edges. Cho et al. [5] used a simplified numerical approach to detect the structural behavior under combined loads. A parametric study was then done to determine the ultimate strength of the stiffened plates under different cases of loading. The results were then studies using regression approach to find the strength formulations, which provided acceptable results with DNV (Plate ultimate limit state) standard and ABAQUS predictions. The aim of Cho's study [5] was to develop formulas that predict the ultimate strength of stiffened plates under the influence of combined axial compression, transverse compression, shear force and lateral pressure loadings.

Ozguc et al. [6] adopted a simple design formula to evaluate the buckling strength of stiffened panels considering both the welding-induced residual stresses and the geometrical imperfections. Formulas were proposed for use in investigation of ship panel geometries using NLFE analysis and validate the results. For instance, Zhang [7] focused on panels under compression and developed a semi-analytical formula to predict ultimate strength under compression (i.e. buckling capacity). Recently, Ozguc [8] utilized the NLFE code named ADVANCE ABAQUS, where an imperfection sensitivity work of a stiffened deck panel on an FPSO vessel is additionally accounted for. In-plane bi-axial compression was explored/studied in two orthogonal directions in the case study. The obtained buckling capacities of the stiffened panels are compared with DNV PULS (Panel Ultimate Limit State) buckling code. The capacities estimate from ADVANCE ABAQUS and DNV PULS code are found to be highly similar.

Though there are several research studies, there is a need for more studies on achieving the calibration of compression of buckling capacities which are obtained by the NLFE method and analytical buckling capacities given in the traditional standards. This is especially important for complex geometries, such as a large ship hull stiffened panels with openings and other irregularities where nonlinearities and geometric deformation are difficult to predict and those have a significant effect on the buckling capacity. However, buckling capacity analysis using NLFE method has few challenges such as (i) introducing applicable geometrical nonlinearities, (ii) identifying issues with material nonlinearity and evaluating the consequences of large strains, (iii) defining boundary conditions that represent the real problem appropriately and (iv) introducing a combined local and global imperfections.

This study aims to apply Nonlinear Finite Element Analysis (NLFE) to assess the buckling capacity in a specific design scenario, specifically, a stiffened panel with substantial openings. Traditional methods do not adequately address this situation. To begin the paper, a stiffened panel with a geometry that can calculate buckling capacity analytically (i.e., using DNV-RP-C201) is chosen. Finite element modeling (FEM) is then conducted for this selected stiffened panel geometry, incorporating nonlinear material properties and accounting for geometric imperfections. The FEM is modified by adjusting the patterns and amplitudes of imperfections, thus yielding buckling capacities. Finally, significant openings are introduced into the nonlinear finite element model of the stiffened panel, and the reduced buckling capacity of the panel due to these large openings is computed.

2. Finite element model description of ship hull stiffened panel
A portion of ship hull stiffened panel (Figure1(a)), which is a geometry commonly used in North Sea, is selected for non-linear buckling analysis. Geometry, material properties, applied loads and boundary conditions, which were used for finite element model description of the selected portion, are described in this section.
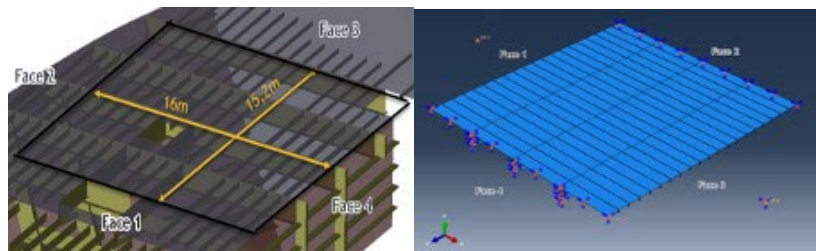
Figure 1. a) Real ship hull stiffened panel model b) FE ship hull model

The selected portion of ship hull stiffened panel, which is a rectangular panel of 15.2 m × 16 m, consists of 19 equally spaced bulb flats stiffeners and three equally spaced girders as shown in Figure 1(a). The geometrical data of the considered panel are shown in Table 1.

Table 1. Geometrical data of FE model

Parameters	Values
(a) Plate	
Plate thickness	15 mm
Plate length	16000 mm
Plate width	15200 mm
(b) Stiffeners geometrical properties	
Profile type	Bulb flats
Number of stiffeners	19
Stiffener length	15200 mm
Stiffener Span	3800 mm
Stiffener spacing	800 mm
Stiffener height	240 mm
Stiffener web thickness	10 mm
Stiffener Bulb width	39.5 mm
Stiffener Bulb thickness	28.8 mm
(c) Girders geometrical properties	
Profile type	Girder T
Number of Girders	3
Girder length	16000 mm
Girder spacing	3800 mm
Girder web height	930 mm
Girder web thickness	12.5 mm
Girder Flange width	450 mm
Girder Flange thickness	30 mm

The material of the panel is S235 and the non-linear material behavior is considered for the analysis. True stress versus strain relation, given by DNV recommended practice, is used for the analysis and non-linear properties of S235 were selected from the same code of practice for thickness less than 16 mm [3].

The boundary conditions and constraints under consideration are illustrated in Figure 1 and summarized in Table 2. To elucidate, a force is applied along the x-axis to Face 1, permitting unrestricted

translation in that direction. In contrast, displacement in the y-direction is restricted to prevent any out-of-plane movement of the plate. Moreover, the plate is assumed to be firmly affixed to a girder at Face 1, thereby constraining rotation around the z-axis (Rz). Face 2, 3, and 4 are assumed to be immovable, as they are connected to both pillars and vertical plates. Displacement in the Z-direction at Faces 1, 2, and 3 is allowed to mimic transverse deformation due to Poisson's effect. Finally, translational displacement along the x-direction at Faces 2 and 4 is unimpeded, as it aligns with the loading direction.

Table 2. FE model boundary conditions

Face	Constrained degrees of freedom
Face 1	Y, Rz
Face 2	Y, Rx, Ry, Rz
Face 3	X, Y, Rx, Ry, Rz
Face 4	Y, Z, Rx, Ry, Rz

3. Non-linear analysis of stiffened ship hull panel using finite element method

Finite element analysis for buckling capacities of geometrically imperfected stiffened ship hull panel is presented in this section in detail. General purpose Finite Element analysis (FEA) program ABAQUS [9] was utilized for this non-linear analysis and the Riks method, which is generally used to simulate geometrically non-linear unstable behavior of structures, was employed. Details of the FE mesh, the considered assumptions the geometrical imperfection and the obtained buckling capacities are presented in this section.

3.1. FE Mesh and assumptions

To conduct the FE mesh, S4R which is a linear quadrilateral shell element was used because shell elements enable specification of the membrane stress components within each element easier. Moreover, the nodes of the element are located at the mid-thickness of each element resulting in no element mesh assigned to the thickness layers [10]. The mesh was generated using the auto meshing tool of ABAQUS. A mesh sensitivity study was performed by few different mesh samples to decide acceptable mesh size to ensure the accuracy of the stress concentrations. Finally, a finite element model meshed with 49703 elements with an average aspect ratio of 1.45 was selected by considering both convergence of the response and computational power.

Furthermore, the assumption used in the analysis are
(i)   perfectly constructed panel before introducing geometrical imperfections,
(ii) straight and continuous stiffeners throughout the girders, which are involved with their full moment capacity on the stiffeners- girders crossing point,
(iii) No buckling in the girders because of the compression stress in the stiffener's direction. This assumption presumes that the girder's function is only to reduce the buckling length of the longitudinal stiffeners and
(iv) perfect contact and stress distribution between the different components of the panel.

3.2. Geometrical imperfection of the panel/model

Perturbations in the geometry was employed to introduce imperfections to the model, while the imperfections were defined by applying linear superposition of multiple eigenmodes. Then the analysis of the eigenmode was done on the ideal structure. Geometrical imperfections were imported using ABAQUS´s built-in features by superposing the weighted mode shapes. Thereafter, the displacements of the nodes from the eigenmode value were multiplied by scale factor to determine the magnitude of the nodes´ coordinate alteration that would provide the desired geometrical imperfections for the non-linear analysis model [9].

The DNV recommended practice [3] provides guidelines to generate geometrically imperfected shapes/patterns based on eigenmodes of the panel. The imperfections patterns recommended by DNV-RP-C208 are divided into global and local imperfections. The local form of imperfections are the out of plane deformation of the plane plate between transverse stiffeners as shown in Figure 2 (left), while the right-hand side figure shows the longitudinal out of plane deformation along the direction on the longitudinal stiffener that are defined as the global imperfections. The recommend imperfection amplitude/values are show in Table 3.
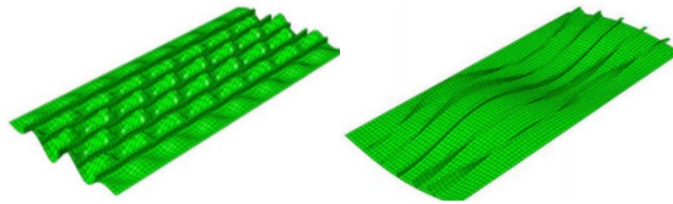

Figure 2. DNV-RP-C208 given local imperfection pattern (left), global Imperfection pattern (right)

Table 3. DNV-RP-C208 imperfection amplitude recommendation [3]

Component	Shape	Magnitude	Imperfection
Longitudinal stiffener girder webs (global imperfection)	Bow	L/400	9.5 mm
Plane plate between stiffeners (Local imperfection)	Eigenmode	S/200	4.0 mm

Note: L stands for length of the girder and S is spacing between transverse stiffeners.

Eigenvalue analysis is performed and three eigen modes patterns were studied as two different cases to determine their patterns and magnitude that can result with the buckling capacity of the calibration benchmark. The eigen modes that provide imperfection patterns similar to the patterns recommended by DNV recommended practice [3] are chosen. Figure 3 shows the pattern of the global imperfection, which is identical for both cases. This imperfection represents the curved bow shape along the stiffener in between the girders.

However, displacement magnitude is not identical at each mid-stiffener span along the panel. Thus, a displacement average amplitude was determined at the middle of the relevant spans indicating the maximum and minimum displacements of the relevant spans. This also helps to have a more realistic case of global geometrical imperfections distribution and magnitude.
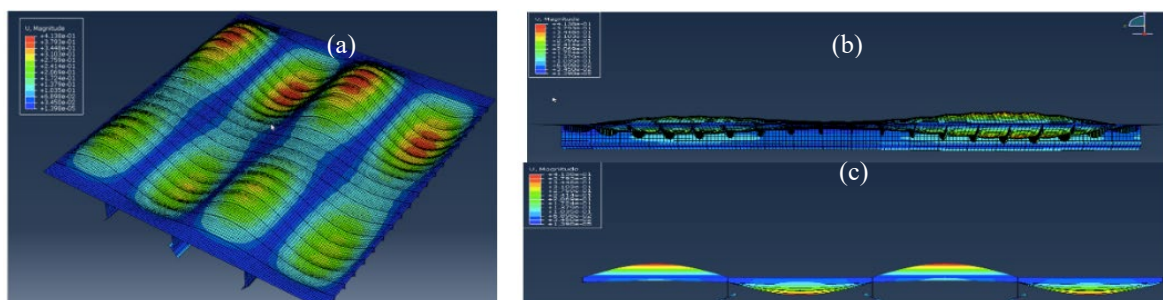

Figure 3. Global imperfection pattern (a) Plate (b) Stiffener side view (c) Girder side view

Figure 4 depicts the local imperfection patterns, which shows the displacement magnitude in the eigenmode at the nodes in the middle plate between the stiffeners. The unequal displacement reveals a more realistic local imperfection distribution. The difference between the two patterns is shown in Figure 3 and Figure 4, where pattern 1 depicts displacements that have sine function shape with the displacement altering to the opposite direction in every sequential stiffener span.

While in pattern 2 (Figure 5), the displacement change direction in every two sequential stiffener span so that the first two stiffener spans have an opposite displacement direction from the last two stiffener spans.
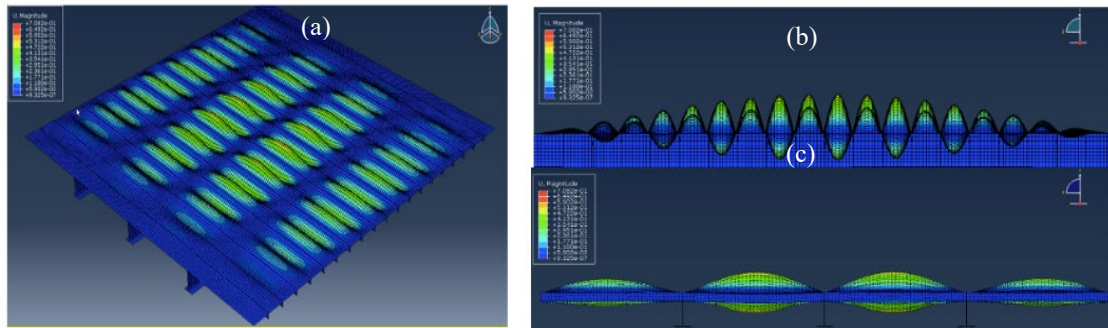

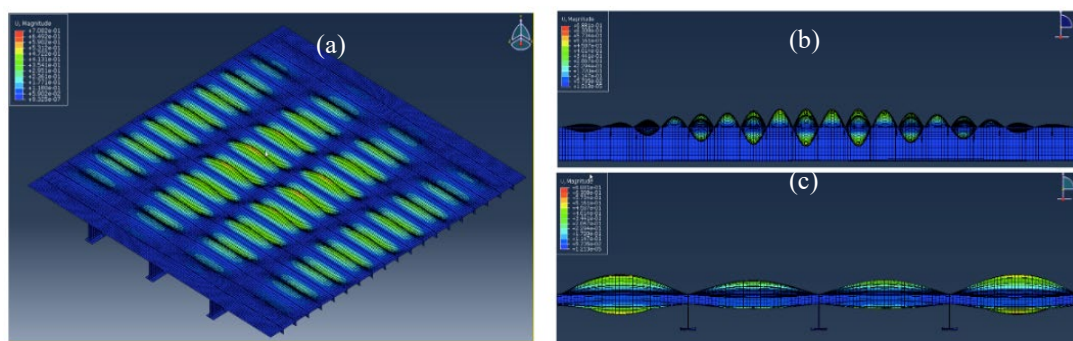**Figure 4.** Local imperfection pattern-1 (a) Plate (b) Stiffener sideview (c) Girder side view

Figure 5. Local imperfection pattern-2 (a) Plate (b) Stiffener sideview I Girder side view

The nodal imperfection, which is the final scaled nodal displacement introduced to the non-linear analysis model from the global and local eigen mode patterns, was obtained using a relation between the scale factor and the nodal displacement as shown below equation.

$$\text{Nodal imperfection} = U_L \times F_L + U_g \times F_G \qquad (1)$$

where nodal imperfection is the final scaled node displacement due to the non-linear analysis model from the global and local eigen mode patterns, U_L is the nodal displacement due to the local pattern, U_g is the nodal displacement due to the global pattern, F_G is Global pattern scale factor and F_L is local pattern scale factor.

The DNV recommended practice [3] provides a minimum mid bow imperfection for the global pattern and mid plate in between stiffeners imperfection as shown in Table 3. Due to the properties of the model geometry properties, the nodes of the global and local patterns obtained from the eigenmode have a wide range of nodal displacement. To apply a scale factor representing a realistic final imperfections pattern in the non-linear analysis model, a study was conducted that can also help to determine the suitable nodal displacement average from each pattern and to determine the scale factor.

The trail scale factor (SF) are found using equation (1), so when multiplied with $U_{L,av,max}$ and $U_{g,av,min}$ the resulting maximum nodal imperfection would be close to U = 13.5 which is the recommended according to DNV-RP-C208 [3].

For each case, three trail Scale Factor (SF) have been found. Two additional SFs were applied to case 1 upon considering the results that will be discussed later. The SF case that results in average of imperfection amplitudes (U_{av}) within the acceptable range results in a buckling capacity close to the benchmark buckling capacity was obtained according to the standards. This was chosen as a calibrated case for the stiffened panel under compression loads. The considered trial SFs are shown in Table 4.

Table 4. Applied scale factors

Case	Imperfection pattern	$U_{av,max}$ (mm)	$U_{av,min}$ (mm)	SF1	SF2	SF3	SF4	SF5
1	Global	0.380	0.1098	47.5	63.63	95	85	77.5
	Local 1	0.410	0.126	18.18	18.18	18.18	18.18	18.18
2	Global	0.380	0.1098	8.9	63.63	95		
	Local 2	0.372	0.128	31.67	18.81	18.18		

3.3. Buckling capacities of imperfected panels

Three non-linear buckling analyses were performed for each scale factor at the combined cases. The obtained results are plotted as force (MN) vs. displacement (mm) of the nodes on Face 1, which is the face where the load is applied. Then the results are compared with DNV-RP-C201, which is hereafter termed as "calibration force". The load versus displacement obtained from FE non-linear analysis are shown in Figure 6 only for both local and global buckling combined cases. In order to establish a calibration capacity, the stiffened panels buckling capacity is determined according to DNV-RP-C201 [1] and considered as a benchmark to calibrate the non-linear finite element model buckling capacity.

ABAQUS combines the local and the global imperfection patterns into one patten of imperfections this is then used in the non-linear analysis. Three non-linear buckling analyses were performed for each scale factor: (1) only local pattern, (2) only global pattern, and (3) the combined case of imperfection pattern. To determine the imperfection case that results in values closest to the reference case provided by DNV-RP-C201, the results are represented as force (MN) vs. displacement (mm) of the nodes in Face 1. The results are shown in Figure 6, Table 5 and Table 6, which are discussed in the next chapter.
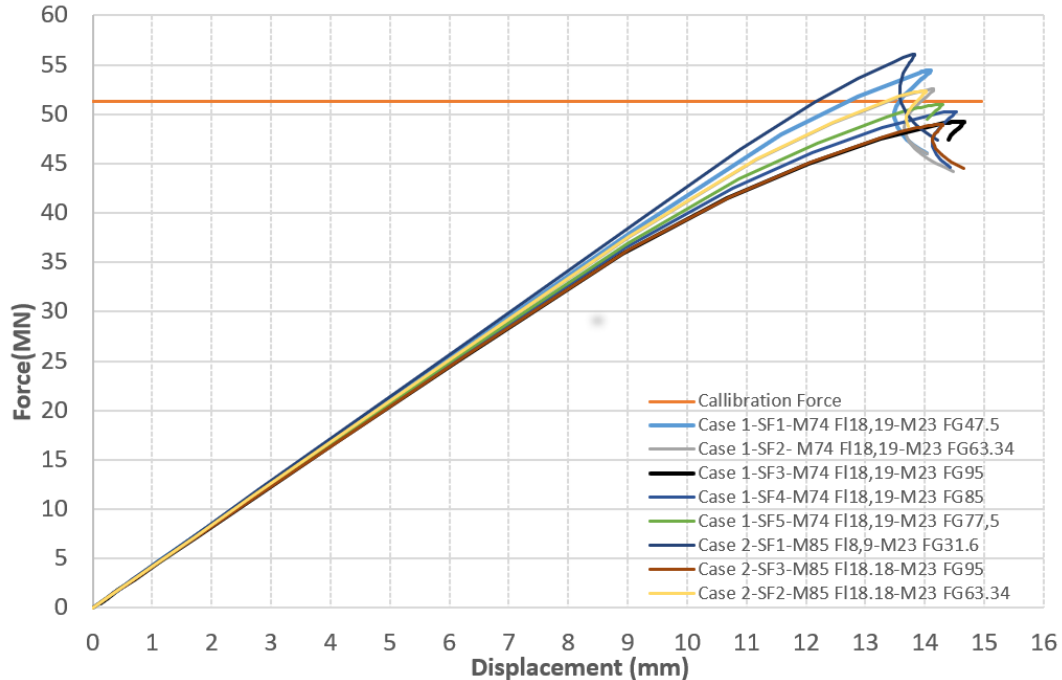

Figure 6. Comparison of the combined patterns cases, nonlinear buckling analysis results

Table 5. Results summary: Nodal Imperfection magnitude of combined imperfection pattern

Case	Imperfection Pattern	Nodal imperfection magnitude of combined imperfection pattern (mm)				
		SF1	SF2	SF3	SF4	SF5
1	Global (M23)[1] Local1 (M85)[2]	5.2-25.6	2.3-31.63	2.29-43.55	2.29-39.75	2.29-36.9
2	Global (M23) Local 2 (M74)[3]	4-11.78	2.4-31.17	2.3-42.89	–	–

Note:
1) M23 is the global pattern eigen mode number.
2) M85 is Local pattern 1 eigen mode number.
3) M74 is Local pattern 1 eigen mode number.

Table 6. Results summary of comparison with reference case

Case	Imperfection Pattern	Diversion to calibration capacity (%)				
		SF1	SF2	SF3	SF4	SF5
1	Global (M23) Local1 (M85)	5.7	+2.3	-4.1	-2.3	-0.58
2	Global (M23) Local 2 (M74)	8.9	+2.09	-4.68	–	–

4. Comparison and discussion

4.1. Comparison of non-linear buckling capacities

To choose the best factors with acceptable imperfection magnitude range along the panel, an educated guess to start with factors that would result in combined imperfection magnitude around double the recommendation of DNV-RP-C208 [3]. For case 1, the chosen scale factor resulted in an imperfection magnitude that range between 5.2 - 25.6 mm along the whole panel. Whereas, for case 2 the range of imperfection magnitude is 4-11.8 mm. Case 2 imperfection range is close to the recommended values in DNV-RP-C208 which is (0 - 13.5 mm) for the investigated panel.

Both those cases gave buckling capacities with a 5.7- 8.9% over estimation of the buckling capacities for this panel. This can be justified by the difference in the shape of the patterns because the global and the local imperfection patterns recommended by DNV-RP-C208 consider an equal imperfection magnitude along the whole panel. The eigen mode analysis of this panel did not provide global or local modes with equal imperfection magnitudes at the mid-spans.

It can be seen from Table 5 that the average imperfection that ranges from SF2 to SF3 are very close in case 1 and 2. This is done to determinate the local imperfection pattern case that gives a buckling capacity closer and under the calibration capacity. As shown in Table 6 and Figure 6, local pattern 1 in case 1 provides a capacity 0.58% closer to the calibration capacity than local pattern 2. This is considering the imperfection contribution of the global pattern, which is the same for both cases. For this reason, case 1 is chosen to continue with the calibration process with SF4 and SF5.

As depicted in Figure 6, SF3, SF4 and SF5 for case 1 and SF3 for case 2 provide estimates of buckling capacity that is lower than the calibration capacity. However, SF3 for case 2 and case 1 provide an underestimate of the capacity of 4.1% and 4.68% while introducing 15% higher imperfection magnitude than SF5 case 1. Also, in case 1, SF4 represents a larger underestimation of the buckling capacity with higher imperfection magnitude than SF5. SF5 in case 1 is thus chosen for calibration cases because it provide only an underestimation of 0.58% of the calibration buckling capacity.

4.2. Calibration of the FE model

The largest imperfection range (31.4 - 37 mm) is concentrated in the middle of the spans 5A,5B, 5C and 5D as illustrated in Figure 7. There is a lower concentration of high imperfections at 7A, 7B, 7C and 7D and 15A, 15B, 15C and 15D due to the global and local patterns of imperfection that intersect with their highest magnitudes at those locations. The highest nodal imperfection of 36.9 mm at middle of the mentioned stiffener spans represents 1% of the stiffener span length. This is higher than the 13.5 mm or 0.355% of the stiffener span length (i.e 3800 mm) which is given in the DNV-RP-C208 [3] recommendation for the case where the maximum imperfections from both patterns intersect. However, the global and the local patterns of imperfection used in the DNV-RP- C208 have equal amplitude of imperfection along the panel. The case was not the same because of the panel geometrical properties and the eigenmode analysis provided global and local patterns of imperfection with different magnitudes along the panel. The von Mises stress distribution along the panel is shown in Figure 8.
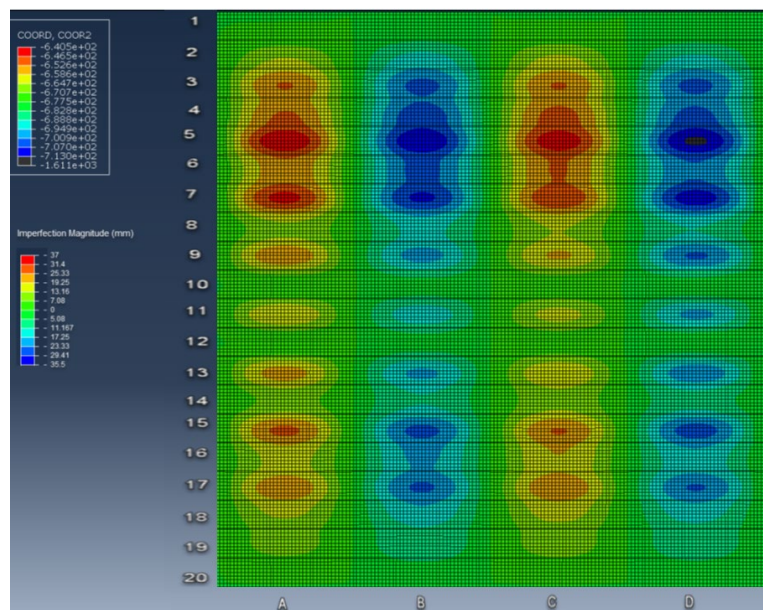

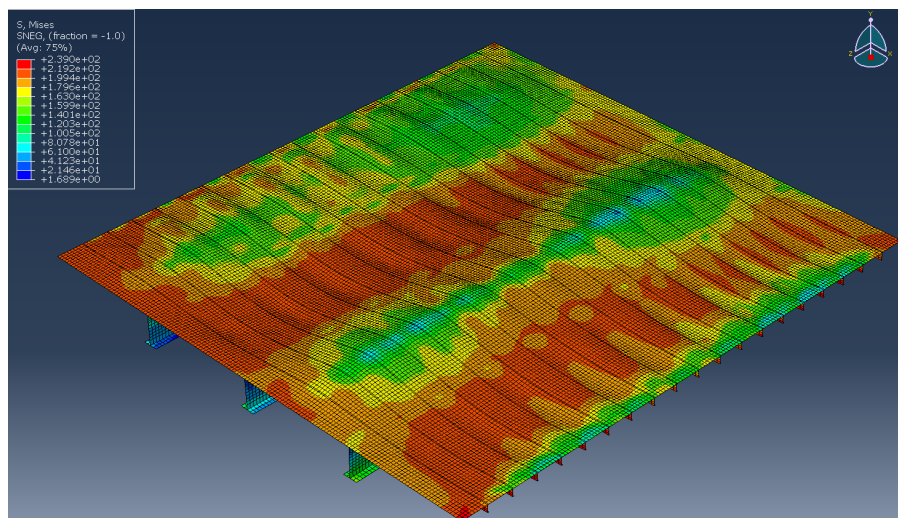**Figure 7.** Calibrated case imperfection magnitude and distribution

Figure 8. Von-mises stress distribution (MPa)

4.3. Parametric study on effect of holes in the panels on buckling capacity
To investigate the effect of holes on the buckling capacity of the model, the several spans were removed as a first step before conducting non-linear buckling analysis. The same imperfection patterns and magnitudes were imposed on the model. Shapes and location of holes 1 and 2 are shown in Figure 9.
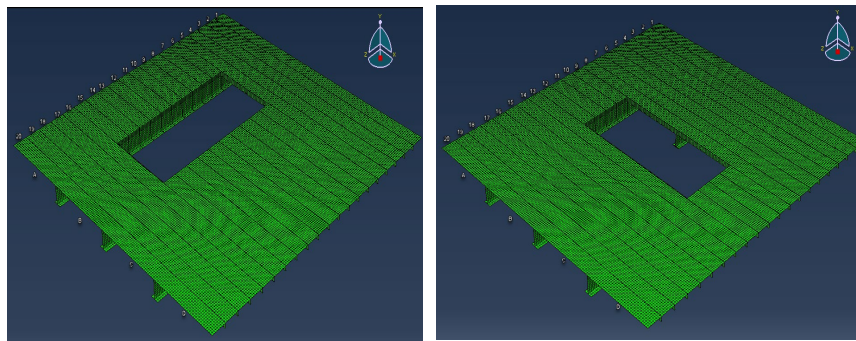

Figure 9. Calibrated model- Hole 1 (left), Calibrated model Hole 2 (Right)

Results of the analysis in Figure 10 and Table 7 display that the percent reduction of the buckling capacity for the calibrated model for hole 1 is almost equal to the span cross sectional reduction, though the area reduction in hole 1 is along spans B and C (Figure 9). The area reduction is related to the area reduction of one stiffener span. This is also the case with hole 2, where the hole is along 10 plates between stiffener spans (stiffener spacing) and one stiffener span (A). The cross-sectional reduction was the governing factor where 50% reduction resulted in 47.8% reduction in the buckling capacity of the model, and 20% reduction resulted in 19.6% buckling capacity reduction.

Table 7. Effects of holes on buckling capacity of the calibrated model

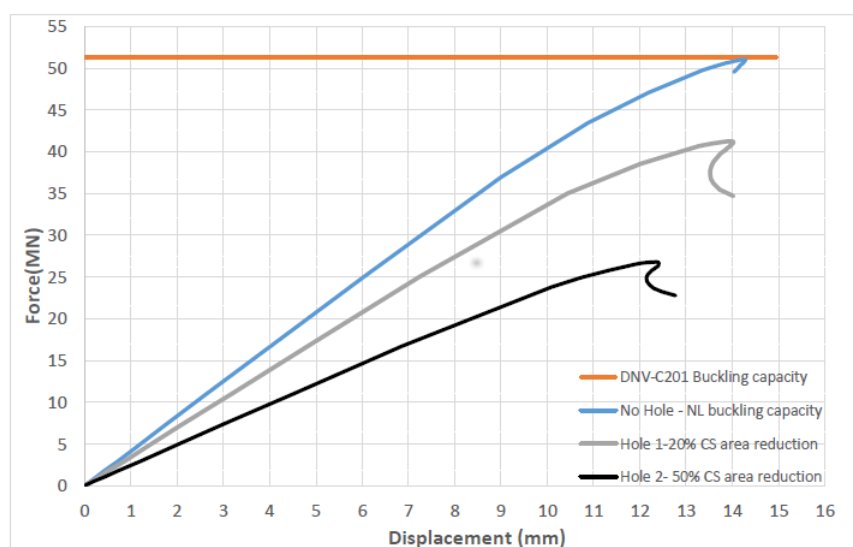|	Area reduction		Results	
	Surface (%)	Stiffener span CS (%)	Buckling capacity (MPa)	Reduction of buckling capacity (%)
Hole 1	10	20	137	-19.6
Hole 2	12.5	50	88.7	-47.8

Figure 10. Effects of holes on buckling capacity of the calibrated model

5. Conclusions

The purpose of this article is to explore the application of a non-linear finite element method as outlined in DNV-RP-C208 [3]. This method is used to assess the buckling capacity of a ship hull stiffened panel. The goal is to then compare and adjust the non-linear buckling capacity with the buckling capacity determined through analytical formulas found in the conventional code DNV-RP-C201 [1]. To achieve this adjustment, the study examines the impact of combinations of one global and two local imperfection patterns, each with various imperfection magnitudes. The selected imperfection patterns closely resemble those recommended in DNV-RP-C208.

The model introduces a mid-stiffener span imperfection magnitude ranging from 0.06% to 1% of the stiffener span length. The aim is to achieve a calibration level of 99.4% with respect to the buckling capacity defined in the DNV-RP-C201 standard. It's noteworthy that the 1% mid-span imperfection magnitude exceeds the DNV's recommended 0.355% of the stiffener span length. This deviation is due to the imperfection patterns derived from eigenmode analysis, which did not provide uniform imperfection magnitudes along the mid-spans of the panel, as assumed in the DNV-RP-C208 recommended patterns. This discrepancy is attributed to the geometric properties and boundary conditions of the panel, as well as the assumption of perfect contact and stress distribution among stiffeners, plates, and girders, which collectively contribute to the larger imperfections introduced for calibration purposes.

With the calibrated non-linear model, the study investigates the influence of holes on the buckling capacity under both uniaxial and gravity loads. The findings demonstrate a reduction in non-linear buckling capacity associated with the reduction in the cross-sectional area of stiffeners and plates caused by the presence of holes in the plate.

As a suggestion for future research, it is recommended to conduct an experimental study on the buckling behavior of a scaled-down version of the same structure under identical loads and boundary conditions. This experimental study would serve to validate the results obtained in this analysis.

References

[1]   DNV Recommended Practice 2010 *Buckling strength of plated structures* DNV-RP-C201, dated October 2010.
[2]   NORSOK standard N-004 2013 *Design of steel structures*, 3rd ed, Norwegian Petroilum Industry.
[3]   DNV Recommended Practice 2021 *Determination of structural capacity by non-linear finite element analysis methods* DNV-RP-C208, Det Norske Veritas, Amended September 2021.
[4]   Paik J K and Thayamballi A K 2003 *Ultimate Limit State Design of Steel Plated Structures*. Chichester, England; Hoboken, NJ: J. Wiley.
[5]   Cho S R, Kim H S, Doh H M and Chon Y K 2013 Ultimate strength formulation for stiffened plates subjected to combined axial compression, transverse compression, shear force, and lateral pressure loadings *Ships Offshore Struct.*, **8**(6), 628–637.
[6]   Ozguc O, Das P K and Barltrop N 2007 The new simple design equations for the ultimate compressive strength of imperfect stiffened plates *Ocean Eng.* **34**, 970–986.
[7]   Zhang S 2016 A review and study on ultimate strength of steel plates and stiffened panels in axial compression *Ships and Offshore Struct.* **11**(1), 81-91.
[8]   Ozguc O 2020 Assessment of buckling behavior on an FPSO deck panel Polish Maritime Research, 27, 50–58.
[9]   Michael S 2009 *ABAQUS/Standard User's Manual* Version 6.9 Providence, RI: Dassault Systèmes Simulia Corp.
[10]   Cook R D, Malkus D S, Plesha M E 1989 *Concepts and Applications of Finite Element Analysis* (4th ed.). New York: Wiley.